JSESM

Journal of Scholastic Engineering Science and Management

March 2022, Volume 1, Issue 1 pp: 38-51

"Mechanical and Experimental Analysis of Air-Flow Supervision Structure Housing in Heat and Air Conditioning System"

[1]Dr.Chandragowda M, [2]Mr. V Sunil, [3]Mr. G. Shankar A, [4]Mr. S. Pratap, [5]Mr.Pratap Gowda B J

[1]Associate Professor, [2,3,4,5]Students (B.E Final Year)

[1,2,3,4,5]Proudhadeveraya Institute Technology, (PDIT), Hosapete, Karnataka, India

Email: [1]chande296@gmail.com

ABSTRACT

Single factor incremental forming (SPIF) is a promising production method appropriate for small batch production. Furthermore, the cloth formability is more advantageous in assessment with the traditional sheet steel forming processes, because of the small plastic area and the incremental nature. Nevertheless, the similarly improvement of the SPIF method calls for the entire information of the cloth deformation mechanism, that is of amazing significance for the powerful method optimization. In this study, a complete finite detail version has been evolved to examine the nation of pressure and pressure withinside the location of the touch area, wherein the plastic deformation will increase by way of the forming device action. The numerical version is first off tested with experimental effects from a easy truncated cone of Al6082T6 aluminum alloy, namely, the forming pressure evolution, the very last thickness and the plastic pressure distributions. In order to assess correctly the through- thickness gradients, the clean is modelled with strong finite elements.

Keywords: *Single Point Incremental Forming (SPIF), Air-Flow, Rectangular Duct*

1. INTRODUCTION

In the sight of growing demands, there are various technical tribulations are commonly being encountered in the meadow of product manufacturing process. So, the need which can be required by the customer could fulfil by an engineer. Keeping in view of this, as an engineer there are various analysis can be done while producing an end product. While analysis and manufacturing of renowned product in an industry, a set of technical family employs various engineers in the vicinity of design, manufacturing, thermal, automation and many more. However, in the vicinity of designing area, various tribulations as well as analysis would consider in order to bring the design model in a required platform. Before taking a look over product designing process, initially the manufacturing process incorporates various basic production processes. Those manufacturing process involves metal casting, metal forming, metal cutting, metal joining and metal finishing process. The assembling scene is in effect further developed and improved step by step. The assembling cycle has been utilized in different structures for a large number of years. Gradual sheet shaping (ISF) measure came into presence to conquer constraint of ordinary framing measure and to handle the prerequisite of high creation rate. Notwithstanding, the significant flaws are long preparing time and non-straight conduct of material that led to multifaceted nature in re-enactment of the ISF cycle. The visual scope of forthcoming utilization of ISF measure is boundless from home to satellite. The single point steady shaping (SPIF) innovation is the mix of framing instrument with a round end wherein the sheet metal is mounted on the installation for the sheet shaping activity. The fundamental point of this work is to give an itemized audit of the individual and interactional impact of cycle boundaries on thickness decrease of SPIF measure. Specific centre is given on impacts of cycle boundaries and the thickness decrease. This paper just presents a plan to advance the new improvement that may likewise go about as a motivation for new specialist. ISF measure as of late is notable as an inventive robotization which promises an advanced adaptability in advancement, lower producing cost, steer time, in aide to upgraded formability of material contended to regular metal shaping cycle.

2. MATERIALS AND METHODS

2.1.Material Design

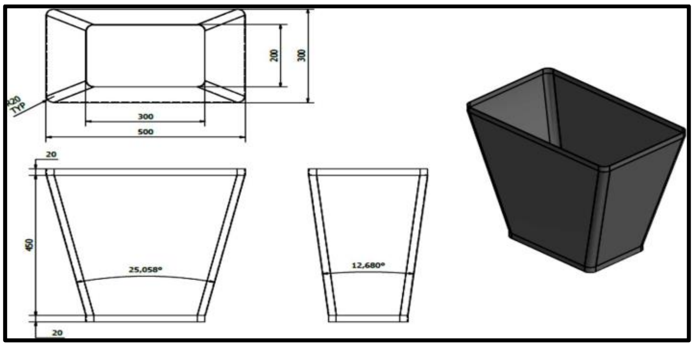

Fig.1.1: Aluminium Al6082T6 Sheet Metal Duc

HVAC of Al6082 T6 is typically supplied as Plate and Sheet.

1) Thickness of Sheet metal = 1.02mm THK
2) Blank Size = 500×300 mm
3) Bottom Blank Size = 300 × 200 mm
4) Yield Strength (K) = 180.39 MPa
5) Density = 2700 km/m3
6) Melting point = 6580C
7) Modulus of Elasticity = 70GPa
8) Tensile Strength = 340 MPa
9) Poisson’s Ratio = 0.3
10) Shear Strength = 210 MPa
11) Elongation = 11%
12) Proof Stress = 310 Mpa

2.2.Material Specifications

- Numerical Analysis accomplished the usage of ABAQUS.
- Section assigned to clean is strong and homogenous.
- Material assigned to clean is T6-6082 Aluminium.
- For SPIF evaluation there may be excessive plastic deformation as a result plastic strain and plastic pressure homes were taken into consideration and implemented.

3. EXPERIMENTAL PROCEDURE

The purpose of the publish processing via way of means of FEM evaluation is to investigate the deformation area that's used for featuring an expression of pace area for the Upper Bound Solution of Incremental sheet steel forming. For studying the deformation area, FEA output of unmarried factor incremental forming evolved via way of means of FEA Package, is used for publish processing.

Simulation of incremental sheet steel forming strategies includes numerous steps as follows:

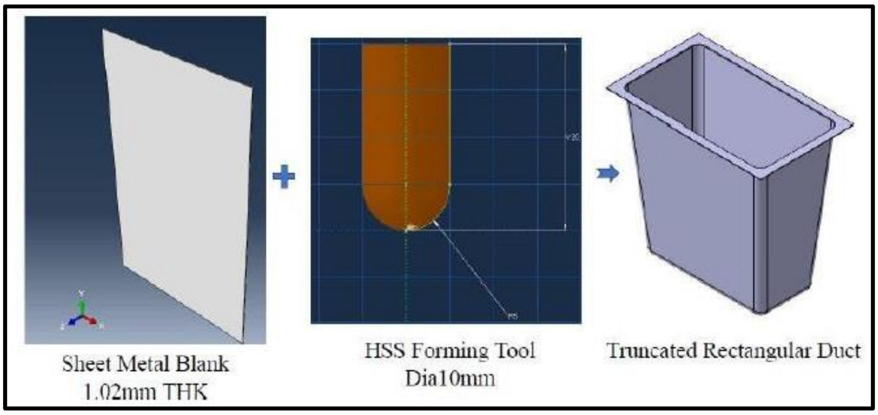

Fig.1.2: CAD model of Aluminium Al6082T6 Sheet Metal Duct and Forming Tool

3.1.Boundary Conditions for Blank

All the faces along the thickness of the blank have been constrained in all DOF

3.1.1. Analytical Computations

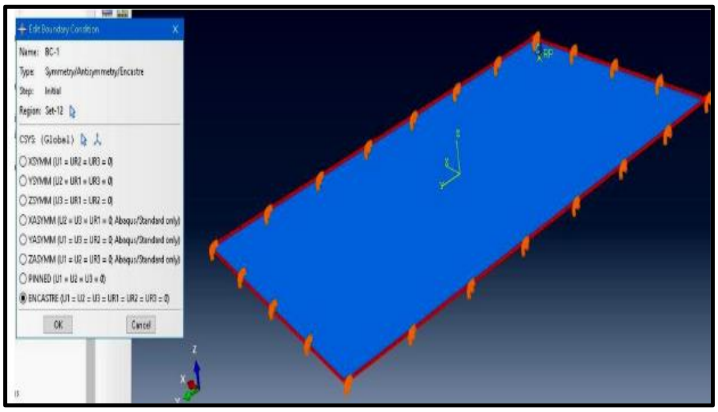

Fig.1.3: Boundary Conditions applied on truncated duct

3.1.1.1.Scrutiny Of the Buckle Machinery In SPIF

To investigate deformation mechanism all through the SPIF process. This evaluation can be finished at the wall-attitude truncated cone simulation.

❖ **Geometry And Material**

Figure suggests a three-D size truncated cone. It is a wall-perspective cone with an intensity of 30 mm. In addition to that geometry, an intensity of turned into extensively utilized for sure results, however the experimental measurements had been now no longer to be had for this intensity. The tool, proven at the proper aspect of the gruel.

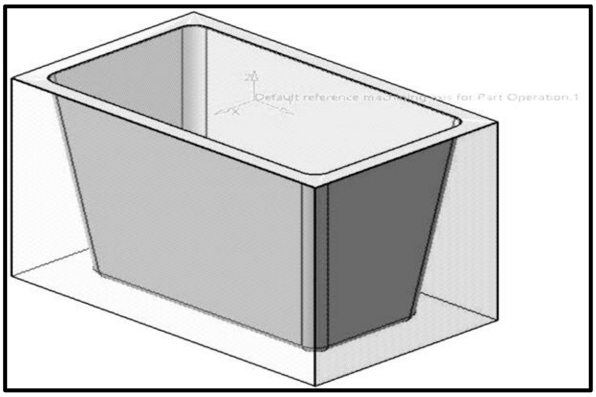

Fig.1.4: Boundary Conditions applied on truncated duct

sheet is 1.02 mm. The wall-attitude of the cone became selected to be 70 stages due to the fact this cost is near the failure attitude, which is set seventy-one stages for this specific alloy and this thickness.

❖ **Meshing Process**

A huge wide variety of simulations were achieved for the duration. code and the era of the enter les may be tedious. numerous Mat lab packages were evolved with a view to assist the consumer with the advent of the meshes and the era of these types of enter les. Two shapes of steel sheets had been typically used for the simulations: rectangular and circular.

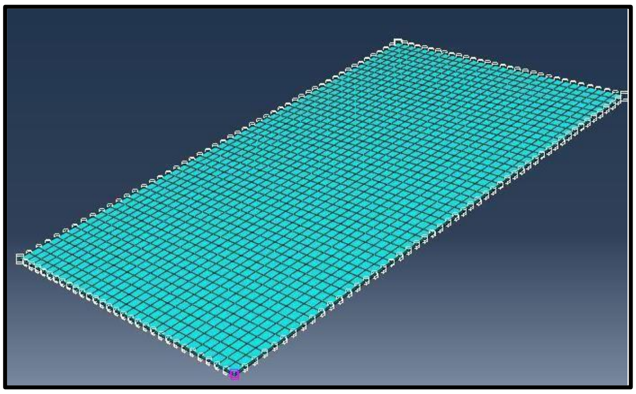

Fig.1.5: Meshing process on duct

❖ **Boundary Conditions for Tool**

Here, U1(X), U2(Y) and U3(Z) is set to 1 respectively to indicate free movement in that direction. 0 indicates fixed Degree of Freedom (DOF). Here, Boundary conditions are applied on the duct element. As shown in the figure 1.6

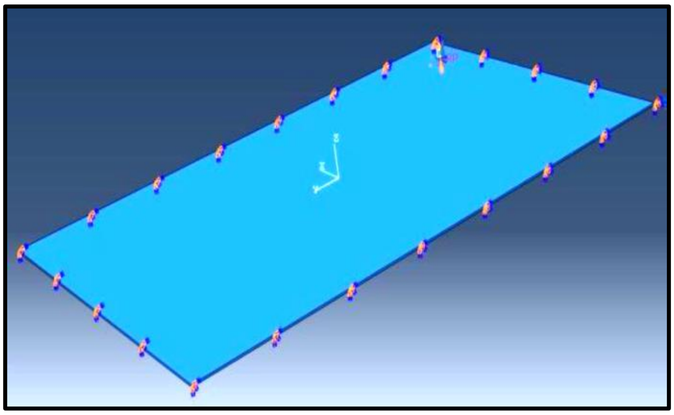

Fig.1.6: Boundary conditions are applied on the duct element

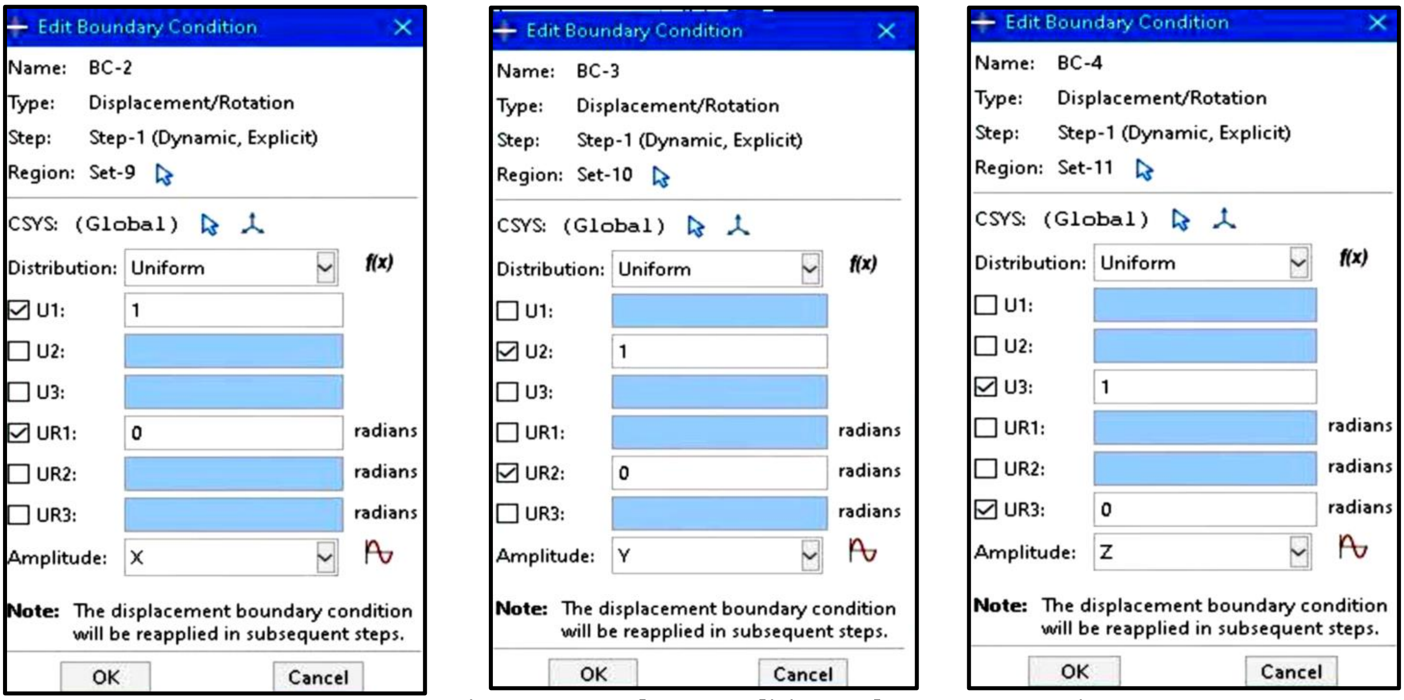

Fig.1.7: Boundary conditions Along X-Y-Z Axis

❖ Tool Path Generation

- ➢ Time Frequency is obtained using above command in MATLAB.
- ➢ Amplitude values are taken from G-Code and M-Code in CATIA V5.
- ➢ Amplitude values represent the co-ordinates of tool movement on blank.

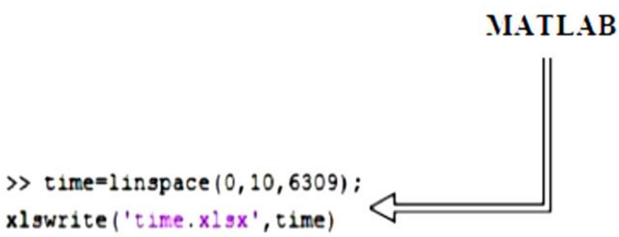

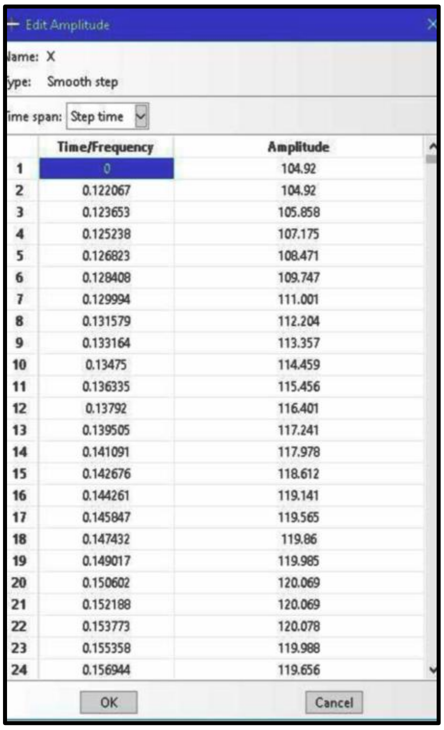

	Time/Frequency	Amplitude
1	0	104.92
2	0.122067	104.92
3	0.123653	105.858
4	0.125238	107.175
5	0.126823	108.471
6	0.128408	109.747
7	0.129994	111.001
8	0.131579	112.204
9	0.133164	113.357
10	0.13475	114.459
11	0.136335	115.456
12	0.13792	116.401
13	0.139505	117.241
14	0.141091	117.978
15	0.142676	118.612
16	0.144261	119.141
17	0.145847	119.565
18	0.147432	119.86
19	0.149017	119.985
20	0.150602	120.069
21	0.152188	120.069
22	0.153773	120.078
23	0.155358	119.988
24	0.156944	119.656

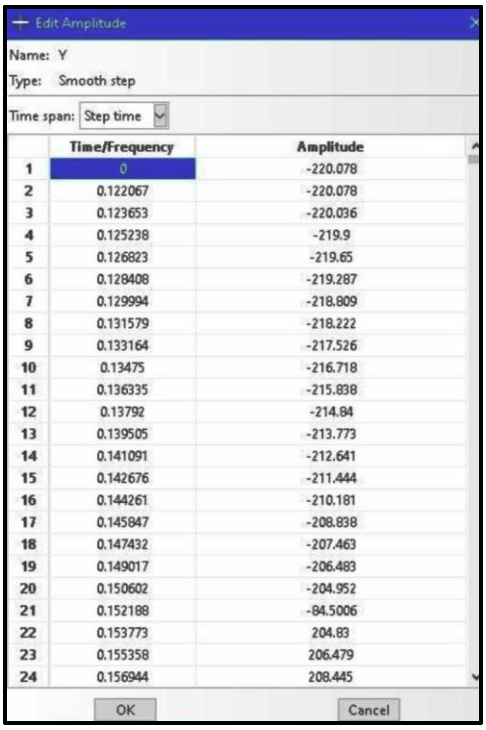

	Time/Frequency	Amplitude
1	0	-220.078
2	0.122067	-220.078
3	0.123653	-220.036
4	0.125238	-219.9
5	0.126823	-219.65
6	0.128408	-219.287
7	0.129994	-218.809
8	0.131579	-218.222
9	0.133164	-217.526
10	0.13475	-216.718
11	0.136335	-215.838
12	0.13792	-214.84
13	0.139505	-213.773
14	0.141091	-212.641
15	0.142676	-211.444
16	0.144261	-210.181
17	0.145847	-208.838
18	0.147432	-207.463
19	0.149017	-206.483
20	0.150602	-204.952
21	0.152188	-84.5006
22	0.153773	204.83
23	0.155358	206.479
24	0.156944	208.445

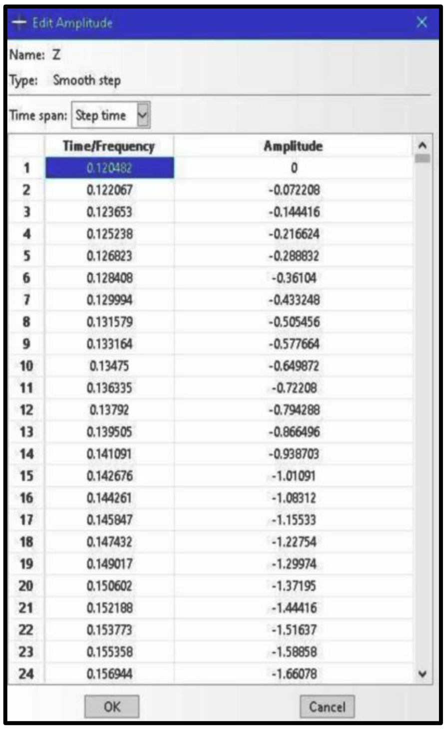

	Time/Frequency	Amplitude
1	0.120482	0
2	0.122067	-0.072208
3	0.123653	-0.144416
4	0.125238	-0.216624
5	0.126823	-0.288832
6	0.128408	-0.36104
7	0.129994	-0.433248
8	0.131579	-0.505456
9	0.133164	-0.577664
10	0.13475	-0.649872
11	0.136335	-0.72208
12	0.13792	-0.794288
13	0.139505	-0.866496
14	0.141091	-0.938703
15	0.142676	-1.01091
16	0.144261	-1.08312
17	0.145847	-1.15533
18	0.147432	-1.22754
19	0.149017	-1.29974
20	0.150602	-1.37195
21	0.152188	-1.44416
22	0.153773	-1.51637
23	0.155358	-1.58858
24	0.156944	-1.66078

Fig.1.8: Tool Path Generation Along X-Y-Z Axis

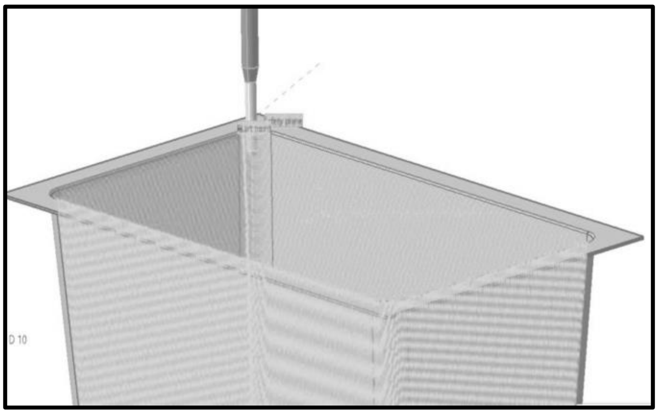

Fig.1.9: Using CATIA V5 Advanced NC Machining Workbench, G-Codes and M-Codes were extracted for the tool path

4. RESULTS AND DISCUSSIONS

Keeping in view of these, there are various discussions are incorporated in this project, with respect to local deformations, strain measurements, stress measurements, counter thickness measurements and many more. In addition to those international predictions, an in-depth evaluation of the conduct of an unmarried detail became performed

Post Processing Results

It is realized that during a selected step body the areas which might be close to through the tool are having a lot greater displacement in comparison to different location.

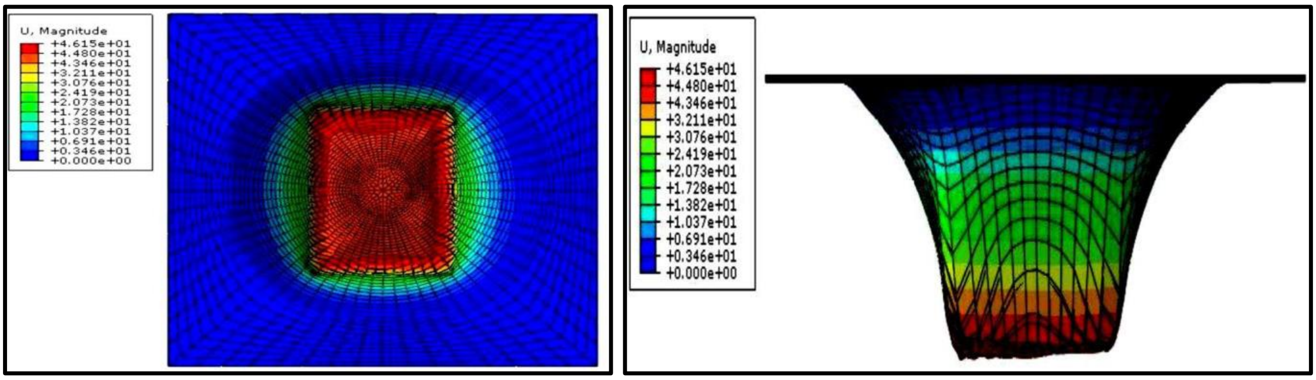

Fig.2.0: Total Deformation rate

4.1.Meridional/Longitudinal Stress S11

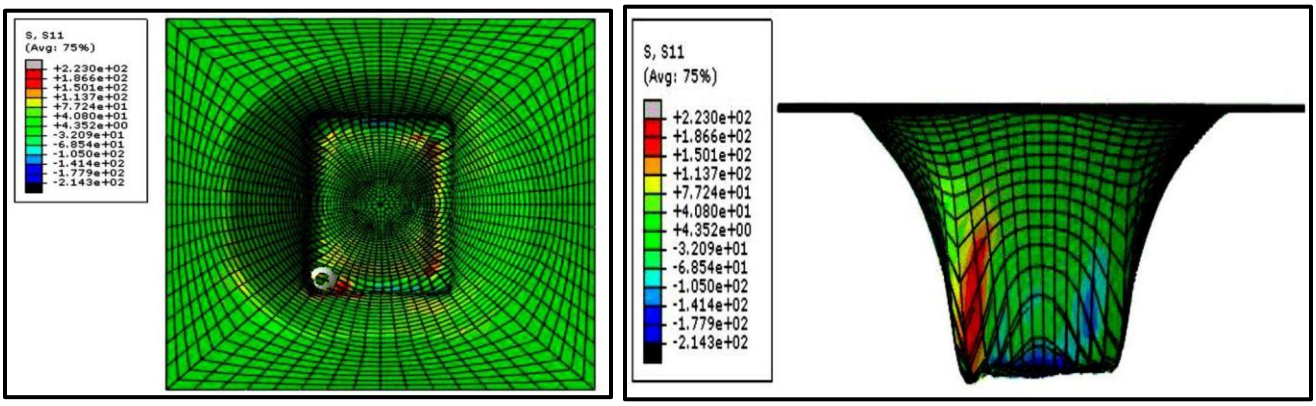

Fig.2.1: Meridional/Longitudinal Stress S11 rate

From Figure 2.1 one can notice that, The magnitude of stress induced is 223 MPa. So, keeping in view of these, the maximum longitudinal stress S11 rate was clinched as 223 MPa.

4.2.Circumferential stress S22

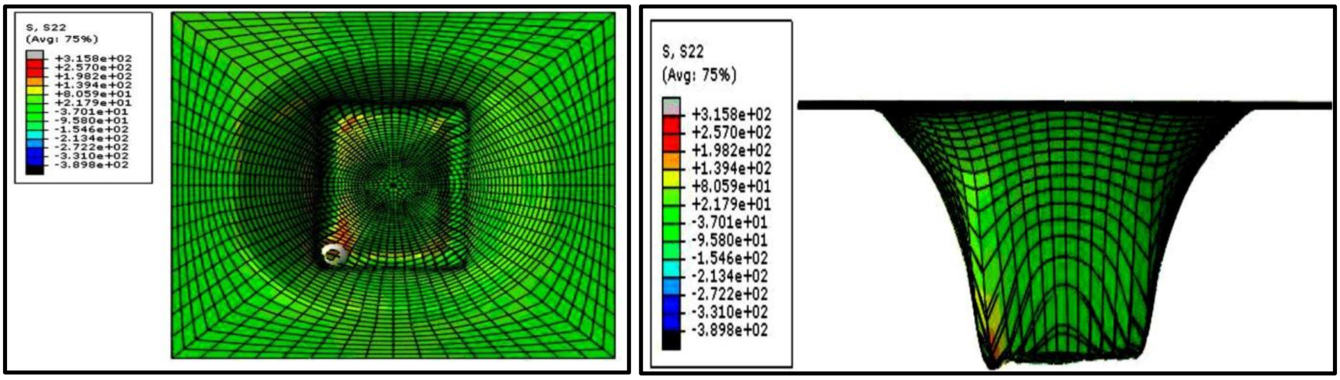

Fig.2.2: Circumferential stress S22

From Figure 2.2 one can notice that, the magnitude of stress induced is 315 MPa. So, keeping in view of these, the maximum longitudinal stress S11 rate was inveterate as 315 MPa.

4.3.Thickness stress S33

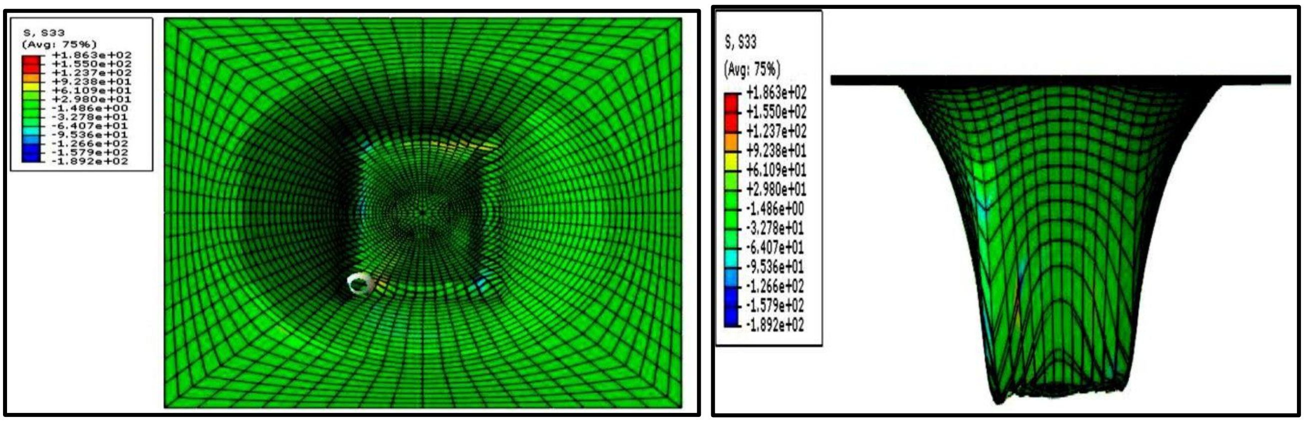

Fig.2.3: Thickness stress S33

It is slightly observed from the figure 2.3, it is clearly noted that, the thickness stress is predominantly The stress induced in the thickness direction is comparatively lower. The magnitude of stress induced is 186 MPa. By considering all the aspects of SPIF process parameters the magnitude of stress induced has been clinched as 186 MPa.

4.4.S11 v/s Forming Depth and Equivalent Strain vs Forming Depth (Plots)

- The stress and strain which is induced throughout the forming depth is indicated in the two plots respectively.
- The peaks are indicative of thinning of stock sheet at that depth of forming.
- It is observed that the peaks are arising at the range when the tool is forming at 30 to 50% depth.

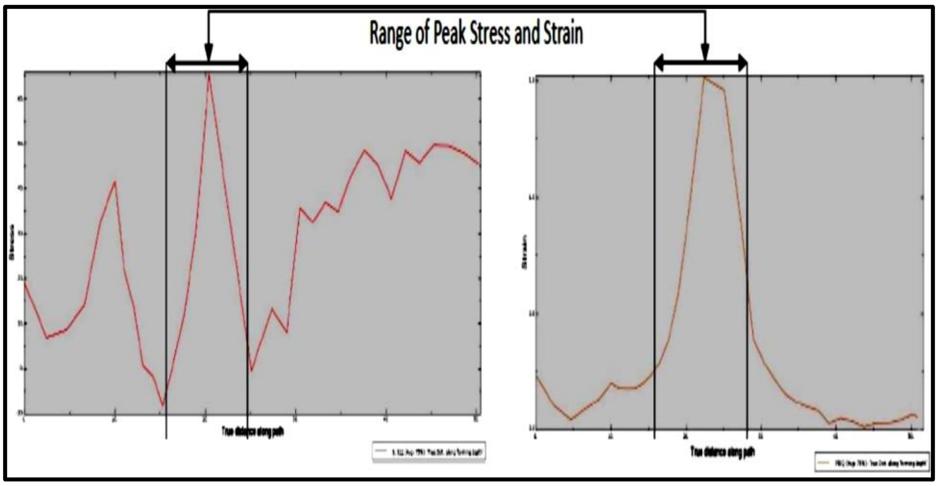

Fig.2.4: S11 v/s Forming Depth and Equivalent Strain vs Forming Depth

4.5.S11 v/s Equivalent Strain (Contours)

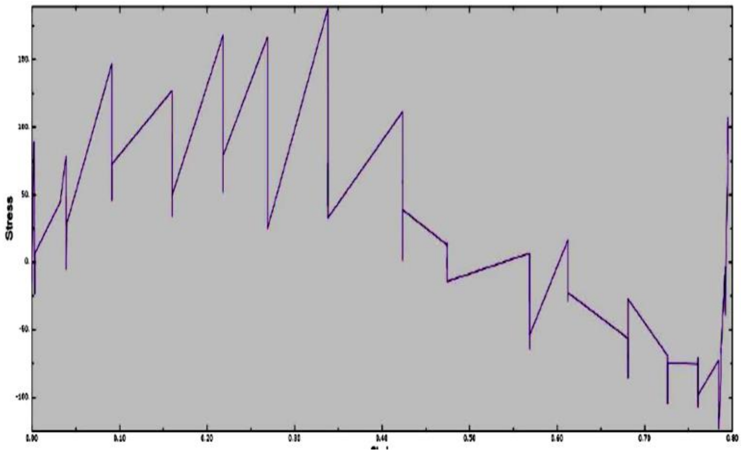

Fig.2.5: S11 v/s Equivalent Strain

Stress vs Strain distribution over the entire forming depth mapping elements that lie on the inner surface of the truncated duct.

4.6.Simulation Progression

After defining all the parameters, eventually the simulation process has carried out. These simulations process has been recorded and the top and side view has been depicted in figure 2.6.

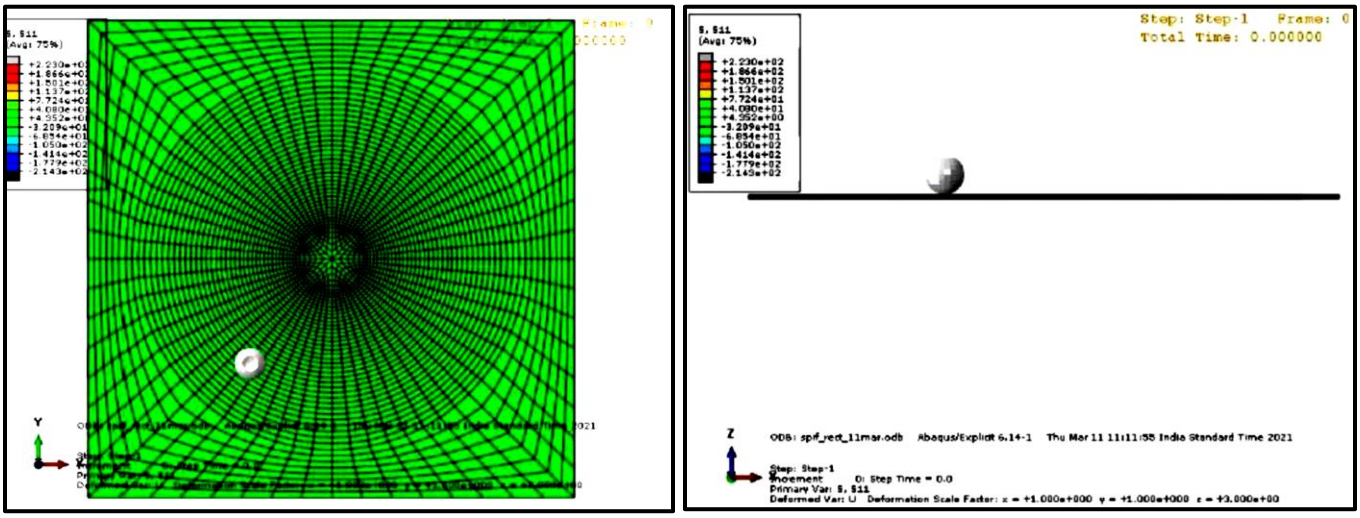

Fig.2.6: Top and Side View of SPIF Simulation Process

CONCLUSION

Eventually, after considering all the aspects of experimental parameters with results, in the present work it is clearly understood.

- Stress magnitude gradually increases with increasing forming depth and with feed rate.
- Time period for tool to travel from top surface to bottom surface is approximately 380sec with computer-based feeding rate (50mm/sec) and CPU consumed time of approximately 15hrs for given parameters for a simulation.

REFERENCES

[1]. Alavala, C.R., 2016. FEM analysis of single point incremental forming process and validation with grid-based experimental deformation analysis. International Journal of Mechanical Engineering, 5(5), pp.1-6.

[2]. Ambrogio, G., Filice, L., De Napoli, L. and Muzzupappa, M., 2005. A simple approach for reducing profile diverting in a single point incremental forming process. Proceedings of the Institution of Mechanical Engineers, Part B: Journal of Engineering Manufacture, 219(11), pp.823-830.

[3]. Arfa, H., Bahloul, R. and BelHadjSalah, H., 2013. Finite element modelling and experimental investigation of single point incremental forming process of aluminum sheets: influence of process parameters on punch force monitoring and on mechanical and geometrical quality of parts. International journal of material forming, 6(4), pp.483-510.

[4]. Duflou, J., Tunckol, Y., Szekeres, A. and Vanherck, P., 2007. Experimental study on force measurements for single point incremental forming. Journal of Materials Processing Technology, 189(1-3), pp.65-72.

[5]. Essa, K. and Hartley, P., 2011. An assessment of various process strategies for improving precision in single point incremental forming. International journal of material forming, 4(4), pp.401-412.

[6]. Eyckens, P., Belkassem, B., Henrard, C., Gu, J., Sol, H., Habraken, A.M., Duflou, J.R., Van Bael, A. and Van Houtte, P., 2011. Strain evolution in the single point incremental forming process: digital image correlation measurement and finite element prediction. International journal of material forming, 4(1), pp.55-71.

[7]. Fang, Y., Lu, B., Chen, J., Xu, D.K. and Ou, H., 2014. Analytical and experimental investigations on deformation mechanism and fracture behavior in single point incremental forming. Journal of Materials Processing Technology, 214(8), pp.1503-1515.

[8]. Ham, M. and Jeswiet, J., 2007. Forming limit curves in single point incremental forming. CIRP annals, 56(1), pp.277-280.

[9]. Henrard, C., 2009. Numerical simulations of the single point incremental forming process.

[10]. Henrard, C., Bouffioux, C., Eyckens, P., Sol, H., Duflou, J.R., Van Houtte, P., Van Bael, A., Duchene, L. and Habraken, A.M., 2011. Forming forces in single point incremental forming: prediction by finite element simulations, validation and sensitivity. Computational mechanics, 47(5), pp.573-590.

[11]. Hmida, R.B., Thibaud, S., Gilbin, A. and Richard, F., 2013. Influence of the initial grain size in single point incremental forming process for thin sheets metal and microparts: experimental investigations. Materials & Design, 45, pp.155-165.

[12]. Hussain, G., Gao, L., Hayat, N. and Ziran, X., 2009. A new formability indicator in single point incremental forming. Journal of Materials Processing Technology, 209(9), pp.4237-4242.

[13]. Jeswiet, J., Micari, F., Hirt, G., Bramley, A., Duflou, J. and Allwood, J., 2005. Asymmetric single point incremental forming of sheet metal. CIRP annals, 54(2), pp.88-114.

[14]. Kurra, S., Rahman, N.H., Regalla, S.P. and Gupta, A.K., 2015. Modeling and optimization of surface roughness in single point incremental forming process. Journal of Materials Research and Technology, 4(3), pp.304-313.

[15]. Li, Y., Daniel, W.J., Liu, Z., Lu, H. and Meehan, P.A., 2015. Deformation mechanics and efficient force prediction in single point incremental forming. Journal of Materials Processing Technology, 221, pp.100-111.

[16]. Malhotra, R., Bhattacharya, A., Kumar, A., Reddy, N.V. and Cao, J., 2011. A new methodology for multi-pass single point incremental forming with mixed toolpaths. CIRP annals, 60(1), pp.323-326.

[17]. Malhotra, R., Xue, L., Belytschko, T. and Cao, J., 2012. Mechanics of fracture in single point incremental forming. Journal of Materials Processing Technology, 212(7), pp.1573-1590.

[18]. Martins, P.A.F., Kwiatkowski, L., Franzen, V., Tekkaya, A.E. and Kleiner, M., 2009. Single point incremental forming of polymers. CIRP annals, 58(1), pp.229-232.

[19]. Micari, F.A.B.R.I.Z.I.O., Ambrogio, G. and Filice, L., 2007. Shape and dimensional accuracy in single point incremental forming: state of the art and future trends. Journal of Materials Processing Technology, 191(1-3), pp.390-395.

[20]. Neto, D.M., Martins, J.M.P., Oliveira, M.C., Menezes, L.F. and Alves, J.L., 2016. Evaluation of strain and stress states in the single point incremental forming process. The International Journal of Advanced Manufacturing Technology, 85(1), pp.521-534.

[21]. Orteu, J.J., Bugarin, F., Harvent, J., Robert, L. and Velay, V., 2011. Multiple-camera instrumentation of a single point incremental forming process pilot for shape and 3D displacement measurements: methodology and results. Experimental mechanics, 51(4), pp.625-639.

[22]. Raju, C. and Narayanan, C.S., 2016. Application of a hybrid optimization technique in a multiple sheet single point incremental forming process. Measurement, 78, pp.296-308.

[23]. Said, L.B., Mars, J., Wali, M. and Dammak, F., 2017. Numerical prediction of the ductile damage in single point incremental forming process. International Journal of Mechanical Sciences, 131, pp.546-558.

[24]. Sbayti, M., Bahloul, R., BelHadjSalah, H. and Zemzemi, F., 2018. Optimization techniques applied to single point incremental forming process for biomedical application. The International Journal of Advanced Manufacturing Technology, 95(5), pp.1789-1804.

[25]. Skjødt, M., Bay, N., Endelt, B. and Ingarao, G., 2008. Multi stage strategies for single point incremental forming of a cup. International Journal of Material Forming, 1(1), pp.1199-1202.